A SIMPLIFIED METHOD TO ANALYZE PILE-SUPPORTED AND GEOSYNTHETIC-REINFORCED EMBANKMENTS AND THE INFLUENCE SIGNIFICANCE ANALYSIS OF THE DESIGN PARAMETERS

Liu Feicheng (corresponding author)
Southwest Jiaotong University,
Ministry of Education,
Key Laboratory of High-Speed Railway Engineering
Chengdu, Sichuan 610031, China
E-mail: liufeicheng@my.swjtu.edu.cn

Zhang Jianjing
Southwest Jiaotong University,
Ministry of Education,
Key Laboratory of High-Speed Railway Engineering
Chengdu, Sichuan 610031, China
E-mail: 13699096139@163.com

Yan Shijie
Southwest Jiaotong University,
School of Civil Engineering
Chengdu, Sichuan 610031, China
E-mail: meiying1995@163.com

Cao Licong
Southwest Jiaotong University,
School of Civil Engineering
Chengdu, Sichuan 610031, China
E-mail: 610554991@qq.com

Abstract

A simplified method for evaluating a pile-supported embankment reinforced with geosynthetic (PGRS embankment) is proposed in this paper. The method takes into account not only the arching effect, the membrane effect of the deflected geosynthetic, and the subsoil reaction, but also the pile head settlement, which makes the method applicable for floating piles, as well as piles seated on a firm soil layer. The settlement of the subsoil surface is considered to consist of two parts: (a) the settlement of the subsoil surface equals that of the pile cap with no deformation in geosynthetic yet; (b) the subsoil surface subsides along with the geosynthetic deforming, and the deflected geosynthetic being considered as catenary shaped. The formula for the maximum differential settlement between the subsoil surface and the piles is worked out by analyzing the force equilibrium of the geosynthetic and the stress-strain relationship of the geosynthetic at the edge of the pile cap. The comparison of the calculated results with the observed data and the six current analytical methods has been implemented to verify the proposed method. The influence of the tensile stiffness of the geosynthetic, compression modulus of soft soil, soft soil thickness, embankment height, internal friction angle of the embankment fill and the pile spacing on the subsoil reaction, the stress concentration ratio (SCR) and the tension of the geosynthetic are investigated using the proposed method. The influence significance of these factors has been investigated using the evaluation theory of binary variance analysis for the non-repeatability tests, which helps optimize the design of the PGRS embankment.

1 INTRODUCTION

The construction of embankments over soft soil with a low bearing capacity and high compressibility becomes increasingly common, while their remains a very challenging task for geotechnical engineers due to over-ranging settlement. In order to improve the soft soil, many methods such as preloading, excavation and replacement, vertical columns reinforcement, vertical drainage and vacuum consolidation are proposed. Each alternative has its own merits and limitations. Piles reinforcement is considered as an effective way on account of the accelerating consolidation of the soft soil, minimizing the total and differential settlements significantly and being suitable for various geological conditions [1], [2]. A conventionally piled embankment construction requires a close pile spacing or a large pile cap to transfer most of the embankment load to piles through the arching effect developed in the embankment fill [3]. In order to improve the load-transfer mechanism and

reduce the differential settlement of the piles and subsoil, a geosynthetic reinforcement is arranged beneath the embankment bottom [4]. Recently, the *PSGR* embankment (*PSGR* embankment) has been widely applied in the construction of embankments over soft soil, and turns out to achieve a good effectiveness [5], [2], [6], [7].

The working mechanisms of the *PSGR* embankment depend on the interactions between the granular fill of the embankment, the piles, the geosynthetic and the subsoil [3], and it is generally considered to rely on the arching effect of the embankment fill, the membrane effect of the deflected geosynthetic and the subsoil reaction. The soil arching effect, as the logical starting point for analyzing the load-transfer mechanisms of the *PSGR* embankment, has been described by some typical models, and these models can be organized into categories [8]: (a) Rigid arch models [9], [10]; (b) limit-state equilibrium models [11], [12], [13], [14]; (c) frictional models [15], [16], [17]; (d) empirical models [18]; and (e) concentric arches models [8]. It has been shown that these methods give different results in terms of the load distribution between the piles and the subsoil [19]. When it comes to the membrane effect of the deflected geosynthetic, the load distribution on the geosynthetic has a strong influence on the calculated strain, several load-deformation expressions of geosynthetic are available in the literature, and can be organized into categories: (a) catenary-shaped under a uniform load [20] (Jones C., 1990); (b) arc-shaped under a uniform load [12], [21]; (c) high-order curve-shaped deformation under a triangular distributed load [14]; (d) high-order curve-shaped deformation under an inverse triangular distributed load [22], [8]. The subsoil reaction has an important influence. BS8006 [18] and Guido et al.'s [10] methods disregard the subsoil reaction, which stays on the safe side in the design for the absence of a subsoil reaction at the most extreme situation. Other current methods take the subsoil reaction into account, which is suitable for most situations and avoids an overdesign of the geosynthetic, and consequently, an unnecessary over-cost.

Most of the current analytical methods are developed by combining one analytical model for the arching effect and one model for the membrane effect, and subsoil reaction based on different simplifying assumptions. Some methods are conceptually and mathematically complex, but the most important is that these methods fail to take the pile-head settlement into account. In reality, however, soft soil may exist under the pile toe and the pile acts as floating pile, thus the settlement of the substrata under the pile toe can play an important role in the mechanisms of load transfer, and should not be neglected.

In addition, some authors discussed the influence of some design factors on the load-transfer mechanisms via their own method and claimed that the working stress of the geosynthetic relies on the complex interaction of fill properties, soft soil properties, and geosynthetic properties [21], [23]. However, the influence significance of these properties on the load-transfer mechanisms are not clear yet, but a distinct understanding of influence significance of those designing factors on the working mechanisms helps to optimize the designing of the *PSGR* embankment.

Therefore, in this study, a new simplified method considering not only the arching effect, the membrane effect, the subsoil reaction, but also the pile-head settlement, is proposed. The tension of the geosynthetic, the subsoil reaction and the load on the pile can be calculated by using the proposed method. The influence of the tensile stiffness of the geosynthetic, the soft soil compression modulus, the soft soil thickness, the embankment height and the internal friction angle of the embankment fill on working the mechanisms has been studied via the proposed method, and then the influence significance of these factors on the working mechanisms has been investigated by the evaluation theory of binary variance analysis of the non-repeatability tests.

2 THEORETICAL DERIVATION

In developing the proposed theoretical method, the following simplifications are used:

(a)   The embankment fill is homogeneous, isotropic.
(b)   There is only one layer of geosynthetic considered in this paper.
(c)   The soft soil and the embankment fill deform only vertically, and there is no relative displacement and slippage between the geosynthetic and subsoil.
(d)   The height of the embankment fill is larger than 0.5 times the pile spacing.

2.1 Arching effect

Based on the arching effect model presented by Low et al. [12], the uniform surcharge q on the embankment surface is taken into consideration and the modified model is employed to analyze the arching effect of the embankment supported by individual square caps. The differential settlement required to develop the soil arching is so small that in this analysis it is implicitly assumed to be adequate for a fully developed arching. The total vertical stress σ_{as} applied on the soft subsoil

between the pile caps without considering the geosynthetic can be obtained using Eq.(1), and σ_{as} is considered as the total vertical load acting on the upper surface of the geosynthetic in the following deduction.

$$\sigma_{as} = \eta \frac{\gamma_s (s-a)(K_p - 1)}{2(K_p - 2)} + \eta$$
$$+ \eta \left(\frac{s-a}{s} \right)^{K_p - 1} \left[q + \gamma_s H - \frac{\gamma_s s}{2} \left(1 + \frac{1}{K_p - 2} \right) \right] \tag{1}$$

where γ_s is the density of embankment fill; s is the pile spacing of the piles; a is the square pile cap width; K_p is the Rankine passive coefficient of the earth pressure, $K_p = (1 + \sin\varphi_s)/(1 - \sin\varphi_s)$; where η is the uniform coefficient allowing for the possible non-uniform vertical stress on the soft ground, which varies between 0.8 and 1.0, here η is considered as 0.9; H is the height of the embankment; q is the uniform surcharge acting on embankment surface; φ_s is the friction angle of the embankment fill, and as for cohesive fill, φ_s should be the equivalent friction angle $\varphi_{equ,s}$ that can be determined by:

$$\phi_s = a\tan\left(\frac{\sigma_v \tan\phi_s + c}{\sigma_v} \right) = a\tan\left(\frac{(\gamma H_s + q)\tan\phi_s + c}{(\gamma H_s + q)} \right) \tag{2}$$

2.2 Subsoil reaction

For a piled embankment reinforced by the geosynthetic, pile caps are generally placed at the top of piles, and the geosynthetic reinforcement is arranged over the pile caps. Conventionally, the geosynthetic is assumed to be located beneath the embankment bottom, and fixed at the pile caps boundary [12], [24], [25]. The tensile strain of the geosynthetic is determined by the settlement of the subsoil surface between the piles, and the maximum tension occurs located at the edge of pile cap [3]. The deflection of one single layer of geosynthetic under the upper loading is shown in Fig.1. The settlement of the subsoil surface between the piles is assumed to consist of two parts: (a) just as Fig.1(a) shows, the settlement of the subsoil surface equals that of the pile cap, with no deformation developed in the geosynthetic yet. The load, σ_{as1}, acting on the upper surface of the geosynthetic is supported by the subsoil alone, and the load supported by the subsoil is denoted as σ_{bs1}, and the settlement, y_1, of the subsoil surface equals the settlement δ_p of the pile caps; (b) just as Fig.1(b) shows, the subsoil surface subsides along with the geosynthetic deforming, while the pile caps do not subside. The load acting on the upper surface of the geosynthetic is supported by the subsoil and the geosynthetic together, and the load
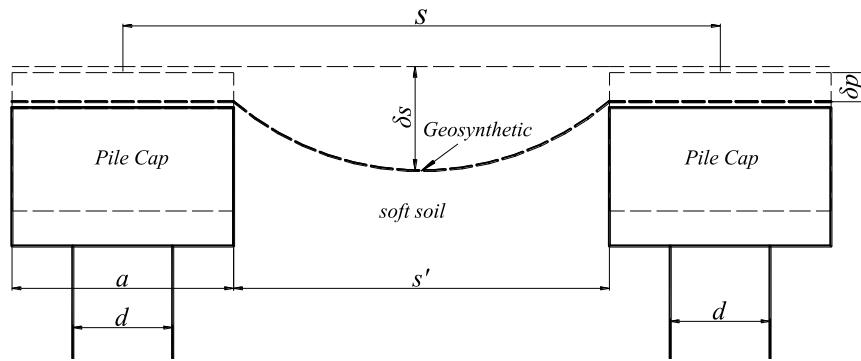

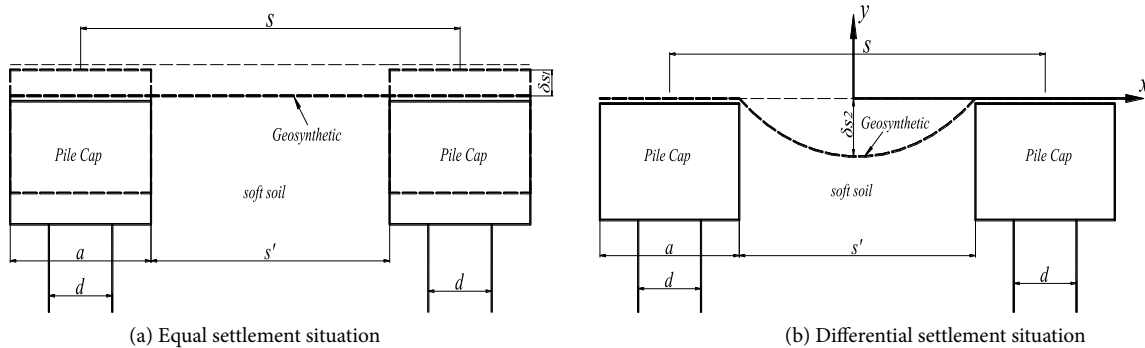**Figure 1**. The total deformation of pile-geosynthetic composite structure.

(a) Equal settlement situation

(b) Differential settlement situation

Figure 2. Sketch of the deformation of the pile-geosynthetic system.

supported by the subsoil is denoted as σ_{bs2}, which causes the settlement, y_2, of the subsoil surface. The total load σ_{bs} acting on the subsoil is the sum of σ_{bs1} and σ_{bs2}.

As Fig.2(a) shows, the settlement of the pile cap is consistent with that of the subsoil, and the geosynthetic is thought to be undeformed, and thus the load σ_{as1} acting on the upper surface of the geosynthetic equals the subsoil reaction σ_{bs1}. The vertical stress σ_{bs1} carried by the subsoil can be given based on a simple equation for the one-dimensional compression of the soft soil:

$$\sigma_{bs1} = -E_s \frac{y_1}{h_s} = -E_s \frac{\delta_p}{h_s} \qquad (3)$$

where h_s is the thickness of soft soil, and E_s is the one-dimensional compression modulus. For multi-layers of soft subsoil, the equivalent one-dimensional compression modulus of the subsoil is expressed as:

$$E_s = \frac{h_s}{h_1 k_1 / E_{s1} + h_2 k_2 / E_{s2} + \cdots + h_n k_n / E_{sn}} \qquad (4)$$

In which, h_1, h_2, ..., h_n are the thickness of each soft soil layer; E_{s1}, E_{s2}, ..., E_{sn} are the one-dimensional compression moduli of each soft soil layer; h_s is the soft soil thickness, which is taken as the sum of the thicknesses of all the soft soil layers.

Fig.2(b) shows the deflection of the geosynthetic, which happens with soft soil being compressed, while the pile caps remain stable. The load σ_{as2} acting on the upper surface of the geosynthetic is uniform, which is supported by the subsoil and geosynthetic together, and can be calculated using:

$$\sigma_{as2} = \sigma_{as} - \sigma_{as1} = \sigma_{as} + E_s \frac{\delta_p}{h_s} \qquad (5)$$

2.3 Membrane effect

The membrane effect of the deflected geosynthetic can be analyzed as an assumed equivalent uniform surcharge, acting on the upper surface of geosynthetic, and the mechanical characteristics of the deflected geosynthetic are shown in Fig.3. The load acting on the upper surface of the geosynthetic equals the load acting on the embankment surface and the moving fill mass gravity, except for the shear resistance of the stationary fill mass, which is undertaken by the geosynthetic and subsoil together. As for the geosynthetic element M, the tension is T, the vertical load on the upper surface of the geosynthetic is σ_{as2} and the subsoil reaction is σ_{bs2}, and the deflection angle to the horizontal direction is θ. Taking the force equilibrium state of the element M, the following equations can be accessed:
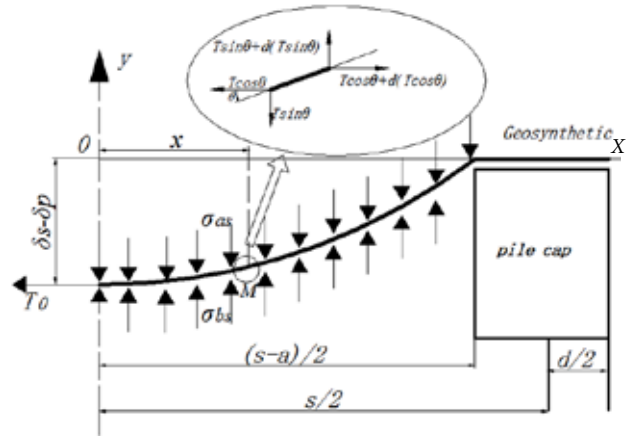

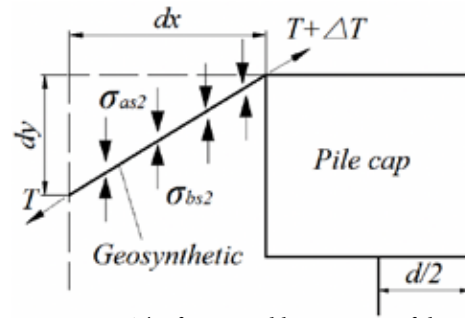**Figure 3**. Mechanical characteristics of the deflected geosynthetic.

Figure 4. The force equilibrium state of the element of geosynthetic.

$$\begin{cases} \sum Fx = 0: & d\left(T\cos(\phi)\right) = 0 \\ \sum Fy = 0: & d\left(T\sin(\phi)\right) = \left(\sigma_{as2} - \sigma_{bs2}\right)dx \end{cases} \qquad (6)$$

where T is the tension of the geosynthetic, and σ_{as2} is the vertical load acting on the upper surface of the geosynthetic, and σ_{bs2} is the subsoil reaction, which varies laterally between the piles and is assumed to be uniform in this analysis.

The horizontal component tension of the geosynthetic is defined to be the constant T_0 under a definite load level. Then, $T \cdot \cos\theta = T_0$, thus $T_0 d(\tan(\theta)) = (\sigma_{as2} - \sigma_{bs2})dx$, $\tan(\theta) = dy_2/dx$, and Eq.(6) can be re-written as:

$$T_0 \frac{d}{dx}\left(\frac{dy_2}{dx}\right) = \left(\sigma_{as2} - \sigma_{bs2}\right) \qquad (7)$$

The tensile strain of the geosynthetic under loads is designed to be so small that the tension is proportional to the strain, and the relationship can be written as:

$$T = J \cdot \varepsilon \qquad (8)$$

where J is the tensile stiffness of the geosynthetic, and ε is the tensile strain of the geosynthetic.

The force equilibrium state of the element with length dx located at the edge of the pile cap is illustrated in Fig.4. The tensile strain of the geosynthetic under tension T is ε, and can be given by:

$$\varepsilon = \sqrt{1+\left(\frac{dy_2}{dx}\right)^2} - 1, \qquad x = \pm\frac{s-a}{2} \qquad (9)$$

According to Jones' research [20], the deformed shape of the geosynthetic under uniform loads is catenary-shaped, and can be described as quadratic parabola:

$$y_2 = ax^2 + bx + c \qquad (10)$$

Taking the boundary condition: When $x=0$, thus $dy/dx=0$ and $y=\Delta\delta$, therefore $b=0$ and $c=\Delta\delta$, and the following equation can be derived:

$$y_2 = ax^2 + \Delta\delta \qquad (11)$$

where $\Delta\delta$ is the differential settlement between the subsoil surface at the midpoint between the piles and the pile cap, and the settlement of the subsoil surface is larger than that of the pile cap, thus $\Delta\delta$ is negative. Taking the boundary condition: When $x=(s-a)/2$, the deflection y of geosynthetic is zero, thus a can be expressed as follows:

$$a = -\frac{4\Delta\delta}{(s-a)^2} \qquad (12)$$

Therefore, the deflection formula of the geosynthetic is expressed as:

$$y_2 = -\frac{4\Delta\delta}{(s-a)^2}x^2 + \Delta\delta \qquad (13)$$

The ultimate deformation formula of the geosynthetic can be expressed as follows:

$$y_{total} = y_1 + y_2 = -\frac{4\Delta\delta}{(s-a)^2}x^2 + \Delta\delta + \delta_p \qquad (14)$$

The first-order and second-order differentiation of Eq.(13) is written as follows:

$$\frac{dy_2}{dx} = -\frac{8\Delta\delta}{(s-a)^2}x \qquad (15)$$

$$\frac{d^2y_2}{dx^2} = -\frac{8\Delta\delta}{(s-a)^2} \qquad (16)$$

Substituting Eq.(16) into Eq.(7), the resulting equation yields:

$$-T_0\frac{8\Delta\delta}{(s-a)^2} = (\sigma_{as2} - \sigma_{bs2}) \qquad (17)$$

The horizontal component tension, T_0, of the geosynthetic can be calculated as follows:

$$T_0 = T\cdot\cos\theta = J\cdot\varepsilon\cdot\cos\theta = J\left(\sqrt{1+(\tan\theta)^2} - 1\right)\cdot\cos\theta = $$

$$= J\cdot\left(\frac{\sqrt{1+\left(\frac{dy_2}{dx}\right)^2}-1}{\sqrt{1+\left(\frac{dy_2}{dx}\right)^2}}\right) \qquad (18)$$

When the deformation is small, the following equation can be obtained by using a Taylor-serious expansion:

$$\sqrt{1+\left(\frac{dy_2}{dx}\right)^2} = 1 + \frac{1}{2}\left(\frac{dy_2}{dx}\right)^2 + \circ\left(\left(\frac{dy_2}{dx}\right)^2\right) \qquad (19)$$

Therefore, the horizontal component tension T_0 of the geosynthetic can be given by neglecting the high-order terms:

$$T_0 = J\cdot\varepsilon\cdot\cos\theta = J\cdot\frac{1}{2\left(\frac{dx}{dy_2}\right)^2+1} \qquad (20)$$

Substituting Eq.(15) into Eq.(20), the following equation yields at the pile edge where x is $(s-a)/2$:

$$T_0 = J\left(2\cdot\left(\frac{(s-a)}{4\Delta\delta}\right)^2 + 1\right)^{-1} \qquad (21)$$

Ultimately, the formula of the subsoil reaction σ_{bs2} yields by combining Eq.(17) and (21).

$$\left(\frac{64J}{(s-a)^4} + \frac{8E_s}{(s-a)^2 h_s}\right)\Delta\delta^3 + \frac{8\sigma_{as2}}{(s-a)^2}\Delta\delta^2 + \frac{E_s}{h_s}\Delta\delta + \sigma_{as2} = 0 \ (22)$$

Until now, the differential settlement of the subsoil surface and the pile cap can be worked out by solving this cubic equation, the maximum settlement of the subsoil surface and the tension of the geosynthetic can be obtained by Eq.(14) and Eq.(21). The total subsoil reaction is obtained by Eq.(23).

$$\sigma_{bs} = -\frac{E_s}{h_s}\left(\Delta\delta + \delta_p\right) \qquad (23)$$

2.4 Pile head settlement

In order to calculate the load acting on the upper surface of geosynthetic σ_{as2}, which is the key to solving Eq.(22), the settlement of the pile δ_p is the primary requirement. The pile head settlement is assumed to include pile tip settlement, the settlement induced by the skin friction of the pile shaft and the compression of the pile shaft. Generally, the compression of the pile shaft can be neglected compared to pile tip settlement and the settlement induced by the skin friction of the pile shaft for its overly large compression stiffness.

2.4.1 Settlement S_b of the pile tip due to the compression of the soft soil beneath the pile tip

The pile tip's resistance and the additional load of the soft soil between the piles are both supposed to be uniformly distributed. Pile tip settlement is dependent on the pile tip's resistance and the additional load acting on the pile tip's horizontal plane between the piles. Just as shown in Fig.5, the settlement of point A is supposed to be induced by the pile tip's resistance σ_{pb2}, the load, σ_{sb2-1}, and σ_{sb2-2}, on the pile tip's horizontal plane between the piles. Therefore, the pile tip resistance and the additional load are the key factors to determine pile tip settlement.
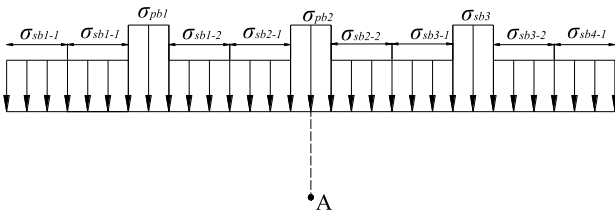

Figure 5. The load distribution at the pile tip's horizontal plane.
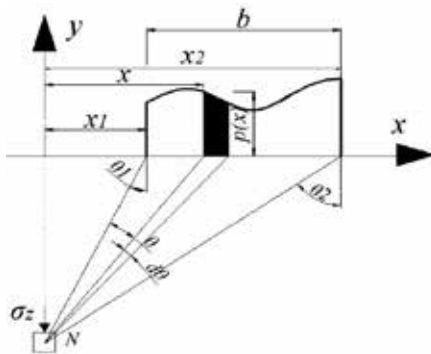

Figure 6. Stress induced by the soil under strip loading.

Yasufuku and Hyde [26] proposed the spherical cavity expansion at the pile tip based on observations from laboratory tests. Therefore, the Vesic Spherical Expansion Theory is employed to calculate the pile tip's resistance. Considering the lateral squeezing due to the interaction of the neighboring piles, the pile tip's resistance can be calculated with the following equation [27].

$$\sigma_{pb} = \sigma_0 \cdot \frac{3(1+\sin\varphi)}{3-\sin\varphi} \left[\left(0.0785\frac{s}{d} - 0.1194 \right) \ln\sigma_0 + \left(0.2593\frac{s}{d} + 0.5426 \right) \right]^{\frac{4\sin\varphi}{1+\sin\varphi}} \quad (24)$$

The load differential of pile head and pile tip is supposed to transfer to the surrounding soil within the reinforced area by the single pile and distributes uniformly. There-

fore, the load increment of the soft soil surrounding the pile can be calculated with:

$$\Delta\sigma_s = \frac{\sigma_{pt}a - \sigma_{pb}d}{s-d} \quad (25)$$

where σ_{pb} is the resistance of the pile tip, σ_{pt} is the load on the pile head and can be given by:

$$\sigma_{pt} = \frac{(\gamma_s H + q)s - \sigma_{bs}(s-a)}{a} \quad (26)$$

According to [28], for the pile group with the center-to-center spacing no larger than six times the pile diameter, the load dispersion along the pile shaft can be neglected, especially at the central part of the pile group. Assuming the subsoil between piles acts as a solid, the load acting on the surface of the subsoil transfers to the pile tip's horizontal plane without any reduction. The additional load acting at the pile tip's horizontal plane between the piles can be calculated approximately with:

$$\sigma_{sb} = \frac{\sigma_{bs}(s-a)}{(s-d)} + \Delta\sigma_s \quad (27)$$

Just as Fig.6 shows, for a point N located at a distance z to the loading surface, the load acting on the range dx is $p(x)$ dx, which can be considered as a concentrated load. The additional vertical stress at point N is $d\sigma_z$ under the load, then the total additional vertical stress σ_z of point N under strip loading is expressed by integrating along the x axis:

$$\sigma_z = \int_{x1}^{x2} \frac{2p(x)dx}{\pi r}\cos^3\theta \quad (28)$$

The settlement S_b of pile tip can then be worked out using the layer-wise summation method.

2.4.2 Settlement S_s induced by the skin friction of the pile shaft

A theoretical solution to the settlement S_s induced by the skin friction of pile shaft was proposed by [29], assuming that the soil surrounding the pile behaves as an elastic, isotropic (Hookean) solid, defined by the modulus of deformation and the Poisson's ratio. For the plane-strain case, the settlement can be given by the following equations.

$$S_s = \left(\frac{P_s}{L}\right)\frac{d}{E_s}(1-\upsilon^2)I_s \quad (29)$$

$$I_s = 2 + 0.35\sqrt{\frac{L}{d}} \quad (30)$$

$$P_s = \sigma_{pt}a - \sigma_{pb}d \quad (31)$$

where p_s is the pile skin friction force; υ is the Poisson's ratio of the soft soil; I_s is the dimensionless influence factor, L is the length of the pile; and E_s is the compres-

sion modulus of soft soil. For multi-layer subsoil the composite compression modulus of the soft soil can be derived using Eq.(4).

2.5 The calculation process

The calculation process is introduced as follows:

(a) The load σ_p of pile head and the load σ_{as} acting on the upper surface of geosynthetic can be obtained with Eq.(1).

(b) The pile head settlement δ_p can be measured by tests, otherwise it can be obtained according to Section 2.2 by taking σ_p as the load acting on the pile head σ_{pt}, and neglecting the effect of the geosynthetic.

(c) The load σ_{as2} can be worked out by substituting σ_p into Eq.(5).

(d) Substituting σ_{as2} into Eq.(22) to calculate the differential settlement $\Delta\delta$.

(e) Substituting $\Delta\delta$. into Eq.(21) to calculate the horizontal component tension T_0 of the geosynthetic.

(f) Substituting $\Delta\delta$ and δ_p into Eq.(14), and the deformation formula of the geosynthetic can be obtained, and the maximum settlement δ_0 of subsoil surface can be worked out.

It is important to note that the soil arch developed in embankment supported by individual caps in the proposed method is analyzed based on the 2d condition, which is normally used when long arches are supported by continuous ledges or cap beams and can achieve good results. Just as Fig.7 shows, the geosynthetic strips act like cap beams, thus the load acting on the geosynthetic strip is noted as Load A, which results from the load transferred by the aching (Load B) and the load transferred by the deflected geosynthetic between four piles (Load C). The geosynthetic strip, supported by two adjacent pile caps, deforms under Load A, and Load A is supported by the deflected geosynthetic strip and the subsoil.

When the embankment height and the clear spacing between the piles is small, considering the support from the subsoil, the deflection of the geosynthetic strip is small, and the load transferred to the pile caps by the deflected geosynthetic strip is small, the stress concentration ratio can be calculated based on the 2d condition. However, when the embankment height and the clear spacing between the piles by the deflected geosynthetic strip is large, the load transferred to the pile caps (Load B and Load C) is high, thus the load acting on the pile caps calculated based on the 2d condition is lower than the measured result, while the calculated result based on the 3d condition is close to the measured one.
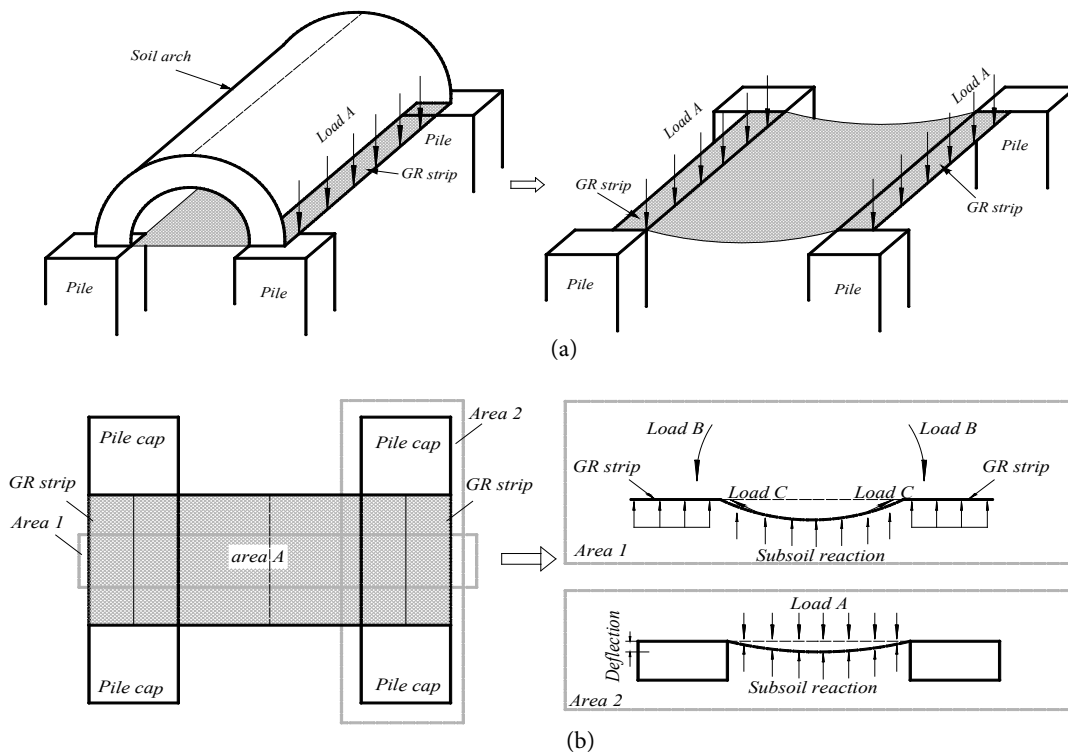

Figure 7. Load-transfer mechanisms of the PSGR embankment.

3 VALIDATION OF THE SIMPLIFIED METHOD

In this section, three embankment cases are employed to verify the proposed method, and then a discussion is presented.

3.1 The Kyoto Road

A case of the *PSGR* embankment is adopted to verify the proposed method. The details of this project, called Kyoto Road, were reported by [6]. The layout of the embankment case is shown in Fig.8, and the main parameters used in the analysis are listed in Table 1.

Table 1. Parameters used in the embankment case.

Param-eters	Unit density (kN/m^3)	Compression Modulus (MPa)	Thickness (m)	Cohesion (kPa)	Friction angle
Embankment fill	18.6	-	1.15	11.5	33.8
Soft soil	-	4.43	8	-	-

Param-eters	Pile spacing (m)	Pile width (m)	Length (m)	Tensile stiffness (kN/m)
Pile/geo-synthetic	1.27	0.3	13.0	1500

The physical and mechanical characteristics of the substratum beneath the pile tip are unknown, and thus the settlement of the pile is hard to estimate. Here the settlement of the pile is neglected for reasons of simplification. The measurements were continued for several years, and a uniform load of 12kPa on the embankment surface is considered to simulate the traffic load. The results measured at 2 years after the construction of the embankment and the calculated results are listed in Table 2. It can be concluded that the results of the proposed method show a good agreement with the measured data.
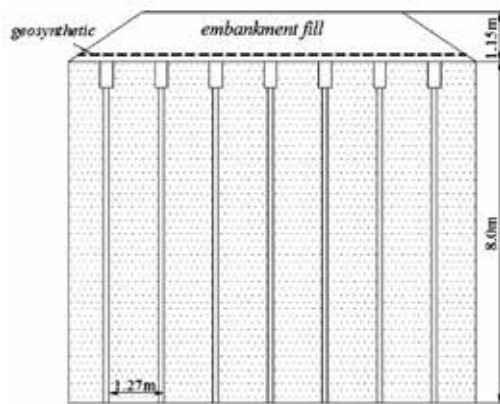

Figure 8. Layout of the embankment case for the Kyoto Road. Drawing modified after Van Eekelen et al., 2008 [6].
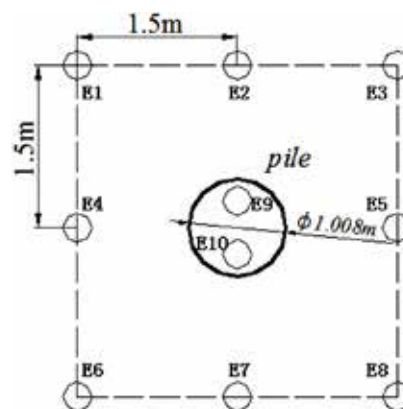

Figure 9. Layout of earth pressure cells of the embankment case of the Shanghai Railway. Drawing modified after Liu et al., 2007 [2].

Table 2. Comparison of the computation results and the field test data.

Param-eters	Load transferring to pile directly by arching effect (kPa)	Vertical load carried by geosynthetic (kPa)	Subsoil resistance (kPa)	Total load on the pile (kPa)
The proposed method	77.6	5.23	16.8	87.3
Field tests	85 (approximately)	4.55	14.0	—

3.2 Shanghai Railway

A *PSGR* embankment case located in the north of Shanghai city, China, was selected to evaluate the proposed method [2]. The embankment height is 5.6m, and the width of the top surface is 35m and that of the bottom is 51.8m. The piles are arranged in a square with 3.0 m for the pile spacing. The dimensions of the pile are: 1.008 m for the outer diameter, 0.12 m thickness and 16 m in length. One layer of an extruded biaxial polypropylene grid was sandwiched between two 0.25-m-thick gravel layers to form a 0.5-m-thick composite-reinforced bearing layer. The tensile strength in both directions is 0.09 MN/m, while the tensile stiffness is 1.18 MN/m. The physical and mechanical parameters of the soil can be found in [23] and [2] and are listed in Table 3.

Fig.9 shows the arrangement of eight earth pressure cells at the subsoil surface and two cells at the pile head. Therefore, the subsoil reaction of the field tests employed here is the average result of these eight earth pressure cells at the ground surface, and the vertical load on the pile head is the average result of the these two earth pressure cells at the pile head. The pile head settlement derived from the proposed method is 19.6 mm, which

Table 3. Mechanical and physical parameters of the soil.

Soil	Thickness (m)	Gravity density (kN/m³)	Compression modulus (MPa)	Poisson ratio	Cohesion (kPa)	Friction angle (°)
Embankment fill	5.6	18.5	—	0.3	10.0	30.0
Silty clay	1.5	—	7.0	0.3	—	—
Soft slity clay	2.3	—	5.0	0.35	—	—
Medium slity clay	10.2	—	3.0	0.4	—	—
Sandy slity	2.0	—	4.0	0.35	—	28.8

is very close to the 19 mm of field tests, which demonstrates the validity of the proposed method in estimating the pile head settlement.

The subsoil reaction and the tension of the geosynthetic is calculated using the proposed method, and then the load acting on the pile head was calculated based on a 3d condition. A comparison of the measured data, the calculated results and the numerical results is shown in Table 4. It can be concluded that the results of the proposed method agree well with those of field tests and the numerical analysis in spite of an overestimation of the load on the pile head by the proposed method. In a word, the proposed method is reasonable.

Table 4. Comparison of results of the proposed method and the field test.

	Load on pile head (kPa)	Subsoil reaction (kPa)	Tension of geosynthetic (kN/m)
Field test	567.9	40.3	—
Calculated results	713.3	43.2	15.9
Numerical analysis	592.6	53.8	16.0

3.3 Comparison with other methods

There are a number of analytical methods available for the analysis of pile-supported and gensynthetic-reinforced embankments. Not all these methods were initially developed to study the gensynthetic-reinforced

and pile-supported embankments, but they were later adopted for this purpose. This section presents a comparison of the proposed method and some other analytical methods.

The geometry of the embankment and the design parameters are obtained from [16] and [20]. Rigid piles with caps and a single layer of geosynthetic were adopted to support the embankment. The relevant parameters used in this analysis are listed in Table 5, and a static surcharge of 12 kPa is applied on the top surface of the embankment to simulate the traffic loading. The calculated results of the embankment are obtained to compare the computed values of the present method with that from several existing analytical methods proposed by [12], [21], [18], [30], [23] and [17].

Based on Eq.(1), the uniform load σ_{as} acting on the upper surface of geosynthetic is 22.10 kPa and the load on the pile head is 61.55 kPa, then the settlement of the pile head is 18.0mm, and then the load σ_{as2} acting on the upper surface of the geosynthetic is 19.44 kPa by Eq.(5), and then the maximum differential settlement $\Delta\delta$ is 68.7 mm by Eq.(22), and thus the horizontal component of tension of geosynthetic, T_0, is 5.54 kN by Eq.(21), and then the load σ_{bs} carried by the subsoil between the piles is derived as 11.73 kPa.

The calculated results using the different methods are listed in Table 6. The tension of the geosynthetic and the load acting on geosynthetic are both over-predicted by [18] for neglecting the support of the subsoil. For this

Table 5. Main parameters of the embankment, pile (cap) and soil.

Components	Parameter	Value	Components	Parameter	Value
	Height (m)	1.39	—	Cap width (m)	1.13
Embankment	Unit density (kN/m³)	20	7.0	Pile spacing/Diameter (m)	2.52/0.6
	Internal friction angle (°)	30		Length (m)	20
	Depth (m)	25	5.0	Compression modulus (MPa)	2.96
Subsoil	Unit density (kN/m³)	17.5	3.0	Internal friction angle (°)	9
	Elastic modulus (MPa)	2.2	4.0	Tension stiffness (kN/m)	1700

Table 6. Comparison of results of different methods.

Parameters	The pro-posed method	Low et al.'s method [12]	Abusharar et al.'s method	BS8006's method [18]	Lu et al.'s method [17]	Zhuang et al.'s method [23]	Van Eekelen et al.'s meth-od [30]
Vertical load on pile (kPa)	72.96	70.92	69.30	71.83	74.85	70.53	71.14
Subsoil reaction(kPa)	12.80	14.50	15.82	0	11.30	14.80	14.32
Tension of geosynthetic(kN/m)	33.23	34.00	39.18	44.40	38.71	23.50	27.76
Vertical load supported by the geosynthetic(kPa)	11.73	14.49	15.81	34.68	19.31	9.73	17.57
Stress-concentration ratio	5.68	4.86	4.38	2.07	6.62	4.76	4.97

embankment case, the embankment height is low, so that the settlement of pile is small, and the influence of the settlement on the calculated results is weak. The results of the proposed method can be found in Table 6, and are in good agreement with [17], [23] and [30], while the proposed method is conceptually and mathematically simpler than these three methods. Even Low et al. [12] and Abusharar et al. [21] assume the deflected geosynthetic as a circular curve, while the proposed method and Lu et al.'s method [17] assume it as parabola-shaped. The tension calculated by different methods shows a good agreement, which demonstrates the slight difference between the two descriptions of the deflected geosynthetic when the deflection of the geosynthetic is small. Lu et al.'s method [17] neglects the pile head settlement, and thus the tension and the load supported by the geosynthetic are both larger than that of the proposed method as a result. Zhuang et al.'s method [23] takes the average horizontal component of the tension instead of the axial tension in the analysis of the force-deformation behavior of geosynthetic, which results in an underestimation of the tension, especially at the edge of the pile cap and the load transferred to the piles by the membrane effect. Van Eekelen et al.'s method [30] underestimates the tension for considering the support of the subsoil by introducing an equivalent subsoil reaction, which allows for the subsoil below the entire geosynthetic area. The vertical load acting on the upper surface of the geosynthetic of the proposed method is less than the equivalent vertical load of Van Eekelen et al.'s method [30], supposing that the load does not rest on the geosynthetic strips between piles transferring to the strips and caps.

3.4 Comparison of several cases

Several field tests (Liu et al., 2007; Chen et al., 2010; Briancon et al., 2012; Van Eekelen et al., 2008; Chen et al., 2008) were selected to be analyzed by the proposed method, just as Table 7 exhibits [2], [31], [7], [6], [32]. These embankment cases in Table 7 can be evaluated by the proposed method with sufficient accuracy,

which demonstrates that the proposed method can be employed to calculate the stress concentration ratio both under 2d and 3dcondition. According to [33], the transfer mechanisms of the load depend on the geometry of the structure (spacing of the pile caps, shape and dimension of the piles caps, height of embankment, etc.), but also the soil characteristics (granularity and mechanical parameters). Chen et al. [32] conducted a series of model tests and concluded that a higher ratio of embankment height to cap beam clear spacing, as well as a higher ratio of cap beam width to clear spacing, would result in a higher stress-concentration ratio. The inclusion of a geosynthetic reinforcement can increase the stress-concentration ratio. In this paper, the ratio of the clear spacing between adjacent piles to the center-to-center spacing is defined as the clear spacing ratio (*NSR*). The ratio of the embankment height to the cap clear spacing is defined as the height spacing ratio (*HSR*).

It can be concluded from Table 7 that like for a pile-supported embankment, without the geosynthetic reinforcement, the stress-concentration ratio is suggested to be calculated based on the 3d condition. The *NSR* is the key factor to be considered, when the *NSR* is low (such as cases 7 and 9), thus the stress concentration ratio is suggested to be calculated based on the 2d condition, and then the *HSR* is the factor deserving consideration, the stress-concentration ratio is suggested to be calculated based on the 2d condition when the *HSR* is low (case 8) and otherwise the 3d condition when the *HSR* is high.(case 1, 5 and 6). Although the proposed method is derived based on the plain-strain condition, using the proposed method to analyze the *PSGR* embankment with individual caps is practicable, and the stress-concentration ratio can be worked out based on the 2d or 3d condition, which depends on the ratio of the clear spacing between the adjacent piles to the center-to-center spacing and the ratio of the embankment height to the cap clear spacing. The influence of the *NSR* and *HSR* is still unclear, and further studies about using the plane arch model to analyze the embankment supported by the individual pile caps are required.

Table 7. The comparison of several embankment cases.

Case number	Pile cap (m)	Geosynthetic J(kN/m)	Embankment height (m)	Pile spacing (m)	2d/3d condition	NSR	HSR
1	No (d=1m)	1180	5.6	3.0	3d	0.67	2.80
2	Square (a=1.3m)	No	6.0	2.5	3d	0.48	5.00
3	Square (a=1.6m)	No	6.0	3.0	3d	0.47	4.29
4	Square (a=1.0m)	No	6.0	2.0	3d	0.50	6.00
5	No (d=0.38m)	800	5.0	2.0	3d	0.81	3.09
6	No (d=0.38m)	800 and 500	5.0	2.0	3d	0.81	3.09
7	Square (a=1.4m)	120	7.2	2.8	2d	0.50	5.14
8	Circular (d=0.3m)	1500	1.15	1.27	2d	0.76	1.19
9	Square (a=1.13m)	1700	1.39	2.52	2d	0.55	1.00

4 PARAMETERS STUDY

The case of the embankment discussed in Section 3.3 is employed to study the influence of the embankment height, the compression modulus of the soft soil, the tensile stiffness of the geosynthetic, the soft soil thickness, the internal friction angle of the embankment fill and the pile spacing on the subsoil reaction, the stress-concentration ratio (SCR) and the tension of the geosynthetic. In this section, these values are used throughout, unless otherwise specified, and the embankment is considered to be supported by cap beams instead of individual caps. No partial factors of safety are applied to the design parameters. The results of this embankment case are illustrated as follows.

4.1 The influence of tensile stiffness of the geosynthetic

The influence of the tensile stiffness on the subsoil reaction is shown in Fig.10. It can be concluded that the subsoil reaction decreases as the tensile stiffness of the
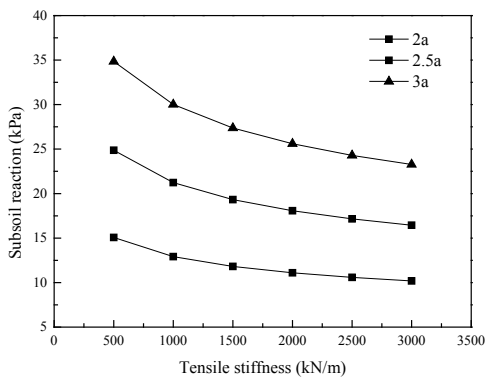
geosynthetic increases, but it is likely to approach a limit value at a large tensile stiffness. The subsoil reaction increases as the pile spacing increases.

Fig.11 shows the influence of the tensile stiffness on the SCR. It can be seen that the SCR increases as the tensile stiffness increases, and is likely to approach a limit value at a large tensile stiffness. The SCR decreases as the pile spacing increases, and the influence at a close pile spacing is slightly more remarkable than that at a large pile spacing. The SCR at a close pile spacing is evidently larger than that at a large pile spacing.
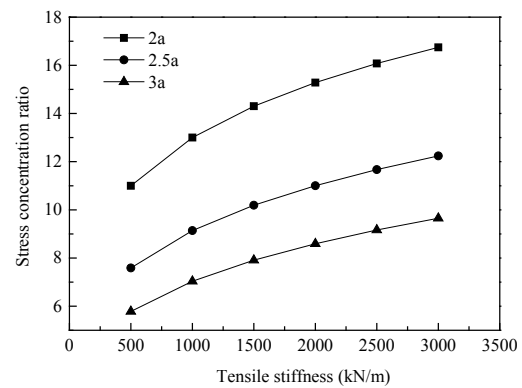

Figure 11. Influence of the tensile stiffness on the SCR.

The influence of the tensile stiffness on the tension of the geosynthetic is exhibited in Fig.12. It can be seen that the tension of the geosynthetic increases as the tensile stiffness of the geosynthetic increases, and tends to approach a limit value at a very large tensile stiffness. The tension differentials between the different pile spacing increases as the tensile stiffness increases. The tension of the geosynthetic at a large pile spacing is larger than that at a close pile spacing.
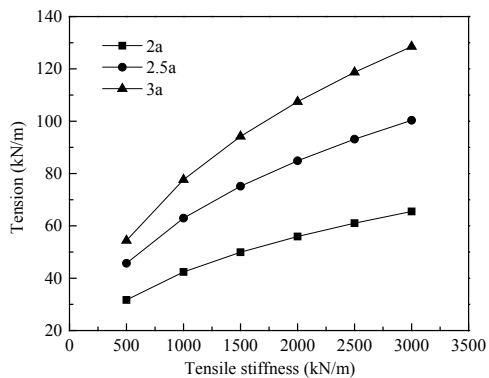

Figure 10. Influence of tensile stiffness on the subsoil reaction.

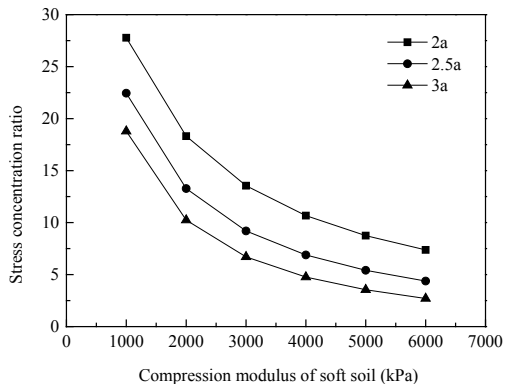**Figure 12**. Influence of the tensile stiffness on the tension.

Figure 14. Influence of the compression modulus on the *SCR*.

4.2 The influence of the soft soil compression modulus

Fig.13 shows the influence of the compression modulus of soft soil on the subsoil reaction. It can be seen that the subsoil reaction increases as the compression modulus increases, and is likely to approach a limit value at a large compression modulus. As the pile spacing increases, the influence of the pile spacing on the relationship of the compression modulus and the subsoil reaction strengthens, and thus the subsoil reaction differentials between the different pile spacing increases evidently as the compression modulus increases.
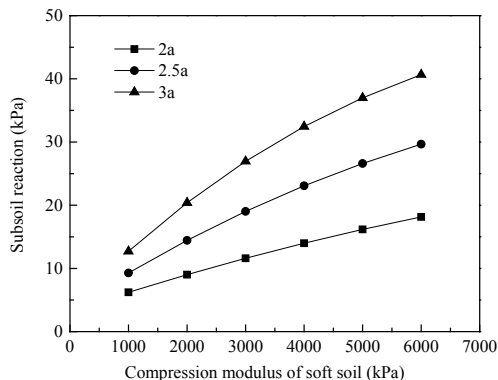

Figure 15. Influence of the compression modulus on the tension.

concluded that the tension of the geosynthetic decreases as the compression modulus increases. The effect of the compression modulus on the tension of the geosynthetic is stronger at a large pile spacing than that at a close pile spacing, and the tensions at different pile spacing are likely to be consistent for a large compression modulus.

4.3 The influence of the soft soil thickness

Fig.16 shows the influence of the soft soil thickness on the subsoil reaction. It can be seen that the subsoil reaction decreases as the soft soil thickness increases, but it is likely to approach the limit value at a large depth. The influence of the soft ground depth on the subsoil reaction at a large pile spacing is stronger than that at a close pile spacing.

Fig.17 shows the influence of the soft soil thickness on the *SCR*. It can be concluded that the *SCR* increases as the soft soil thickness increases. The influence of the soft ground depth on the *SCR* at a close pile spacing is stronger than that at a large pile spacing, thus the *SCR* differentials of the different pile spacing increase as the soft soil thickness increases.

Figure 13. Influence of the compression modulus on the subsoil reaction.

Fig.14 shows the influence of the compression modulus of the soft soil on the *SCR*. It can be concluded that as the compression modulus increases, the *SCR* decreases to a limit value at a large compression modulus. The influence of the pile spacing on the relationship of the compression modulus and the *SCR* enhances with the decreasing of the pile spacing.

Fig.15 shows the influence of the compression modulus of the soft soil on the tension of the geosynthetic. It can be
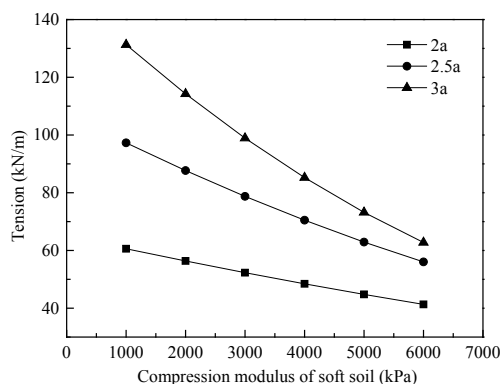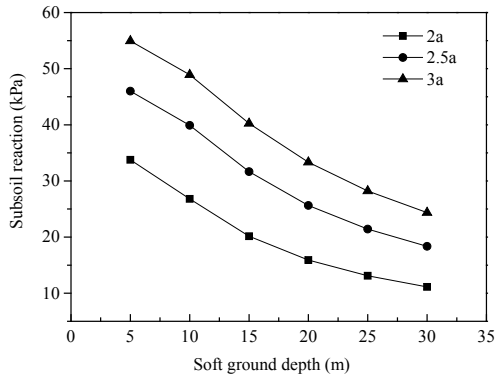
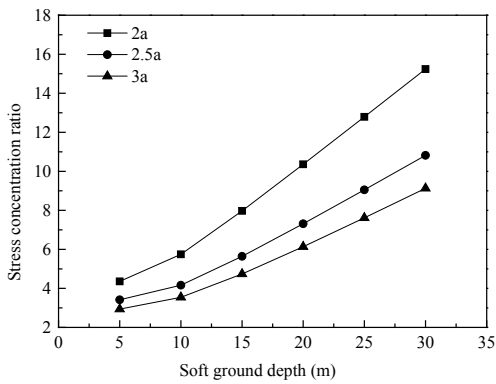**Figure 16**. Influence of soft ground depth on the subsoil reaction.

Figure 17. Influence of soft ground depth on the *SCR*.

Fig.18 shows the influence of the soft soil thickness on the tension of the geosynthetic. It can be seen that the tension of the geosynthetic increases gradually as the soft soil thickness increases, but it is likely to approach the limit value at a large soft soil thickness. The influence at a large pile spacing is obviously stronger than that at a close pile spacing, and the tension differentials between the different pile spacing increase as the soft soil thickness increases.
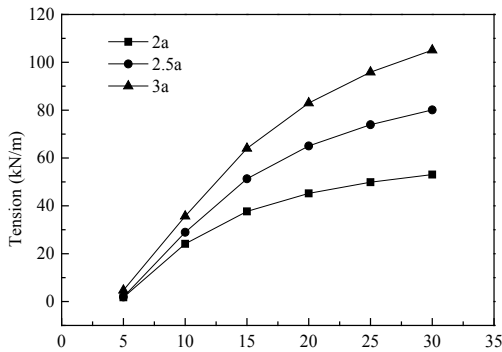

Figure 18. Influence of the soft ground depth on the tension.

4.4 Influence of the embankment height

Fig.19 presents the influence of the embankment height on the subsoil reaction. It can be concluded that the subsoil reaction increases obviously as the embankment height increases. The subsoil reaction is more sensitive to the changing of the embankment height at a large pile spacing than that at a close pile spacing.
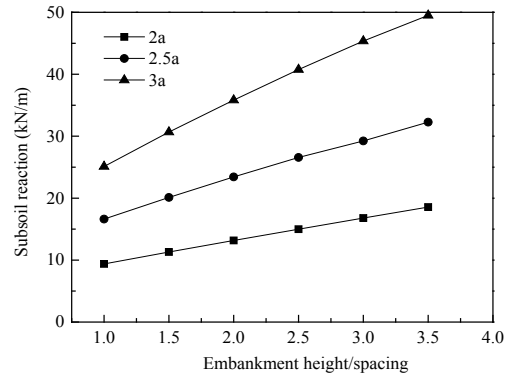

Figure 19. Influence of the embankment height on the subsoil reaction.

Fig.20 shows the influence of the embankment height on the *SCR*. It is clear that the *SCR* increases as the embankment height increases. The influence of the embankment height on the *SCR* is stronger at a close pile spacing than that at a large pile spacing, but the difference of the influence is slight.
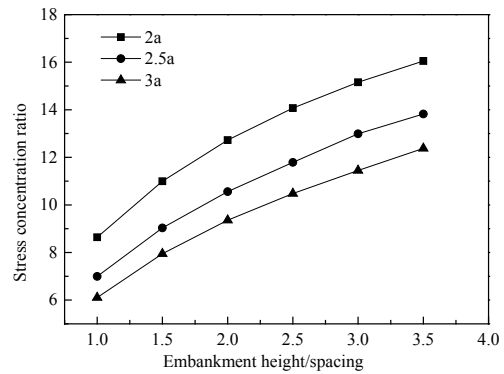
Figure 20. Influence of the embankment height on the *SCR*.

Fig.21 displays the influence of the embankment height on the tension of the geosynthetic. It is obvious that the tension of the geosynthetic increases as the embankment height increases and the pile spacing imposes an evident influence on the relationship between the tension of the geosynthetic and the embankment height. The influence of the embankment height on the tension is clearly stronger at a large pile spacing than that at a close pile spacing, which means the increasing of the embankment
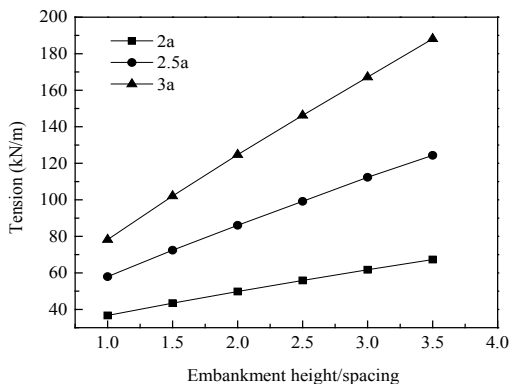
Figure 21. Influence of the embankment height on the tension.

height increases the tension differentials of the geosynthetic at different pile spacings.

4.5 Influence of the internal friction angle of the embankment fill

Fig.22 shows the influence of the internal friction angle of the embankment fill on the subsoil reaction. It can be concluded that the subsoil reaction decreases as the internal friction angle of the embankment fill increases, but it is likely to approach a limit value at a large internal friction angle. The influence at a large pile spacing is stronger than that at a close pile spacing.
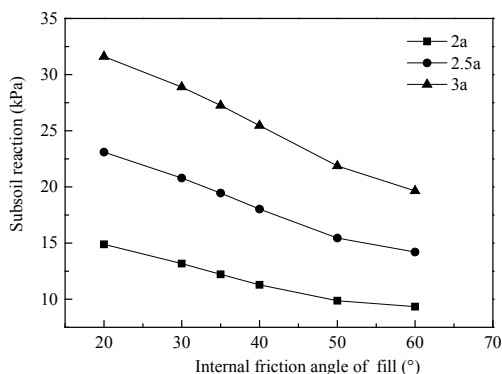

Figure 22. Influence of the internal friction angle on the subsoil reaction.

Fig.23 shows the influence of the internal friction angle of the embankment fill on the *SCR*. It can be seen that the *SCR* increases with the increase of the internal friction angle, but is likely to approach a limit value at a large internal friction angle. It is clear that the influence at a close pile spacing on the relationship between the *SCR* and the internal friction angle is stronger than that at a large pile spacing.

Fig.24 shows the influence of the internal friction angle of the embankment fill on the tension of the geosyn-
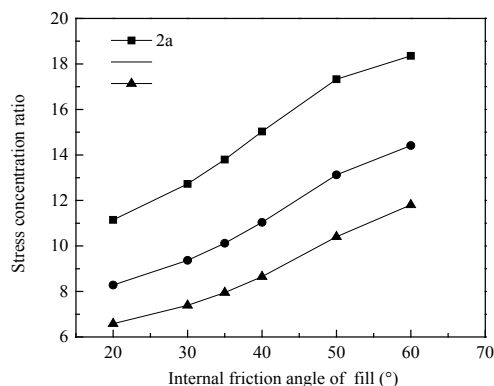
Figure 23. Influence of the internal friction angle on the *SCR*.
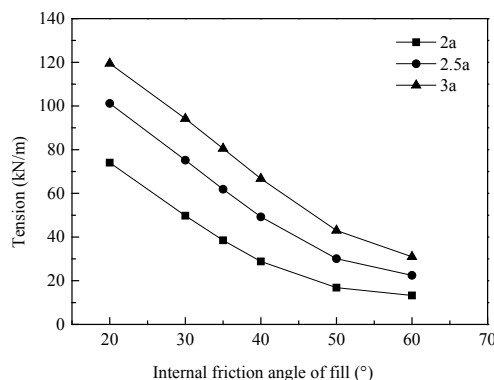
Figure 24. Influence of the internal friction angle on the tension.

thetic. It is clear that the tension of the geosynthetic decreases with the increasing of the internal friction angle, but it is likely to approach to a limit value at a large angle. Obviously, the influence of the internal friction angle on the tension at a large pile spacing is stronger than that at a close pile spacing, and the tension differentials between the different pile spacing decrease as the angle increases.

5 BINARY VARIANCE ANALYSIS OF THE NON-REPEATABILITY TESTS

5.1 Evaluation theory of the binary variance analysis of the non-repeatability tests

The evaluation theory of the binary variance analysis of the non-repeatability tests is a statistical method to assess the influence significance of each factor, the detail analysis process is introduced by [34] and are reported as follows: Assuming that the test result X is influenced by two factors, A and B, and the factor A can be taken as A_1, A_2, ..., A_r, and the factor B can be taken as B_1, B_2, ..., B_s. The test result of A_i and B_j is recorded as X_{ij}, i=1, 2, ..., r; j=1, 2, ..., and test results are mutually independent. The special test process is listed in Table 8.

Table 8. Comparison of the computation results and the field test data.

Factor A	Factor B				X_i
	B_1	B_2	……	B_s	
A_1	X_{11}	X_{12}	……	X_{1s}	$\overline{X1.}$
A_2	X_{21}	X_{22}	……	X_{2s}	$\overline{X2.}$
……	……	……	……	……	……
A_r	X_{r1}	X_{r2}	……	X_{rs}	$\overline{Xr.}$
$\overline{X.j}$	$\overline{X.1}$	$\overline{X.2}$	……	$\overline{X.s}$	$\overline{X}$

The total sum of the squares is expressed as:

$$SST = \sum_{i=1}^{r}\sum_{j=1}^{s}\left(\overline{X_{ij}} - \overline{X}\right)^2 \qquad (33)$$

The sum of the squares for factor A can be expressed as:

$$SSA = s\sum_{i=1}^{r}\left(\overline{X_{i.}} - \overline{X}\right)^2 \qquad (34)$$

The sum of the squares for factor B can be expressed as:

$$SSB = r\sum_{j=1}^{s}\left(\overline{X_{.j}} - \overline{X}\right)^2 \qquad (35)$$

The sum of the squares for random variance can be expressed as:

$$SSE = \sum_{i=1}^{r}\sum_{j=1}^{s}\left(\overline{X_{ij}} - \overline{X_{i.}} - \overline{X_{.j}} + \overline{X}\right)^2 \qquad (36)$$

The freedom degree of the sum of squares for each factor can be expressed as follows: $f_{SST}=IJ-1$; $f_{SSA}=I-1$; $f_{SSB}=J-1$; $f_{SSE}=(I-1)(J-1)$.

In order to quantify the influence significance of factor A, the following equation is adopted:

$$F_A = \frac{SSA/(I-1)}{SSE/\left[(I-1)(J-1)\right]} = \frac{MSSA}{MSSE} \qquad (37)$$

Generally, as for the F-distribution, once a constant value of α is given, the influence of one factor A is considered to be remarkable when F_A is larger than $F_\alpha((I-1), (J-1))$.

The equation to quantify the influence significance of the factor B is written as:

$$F_b = \frac{SSB/(I-1)}{SSE/\left[(I-1)(J-1)\right]} = \frac{MSSB}{MSSE} \qquad (38)$$

Table 9 is an analysis table of the binary variance of the non-repeatability tests, which contains these pre-mentioned items.

Table 9. Binary variance analysis of the non-repeatable tests.

Source of variance	Sum of squares	Degree of freedom	Mean square	F
Main effect of factor A	SSA	I-1	MSSA	F_A
Main effect of factor B	SSB	J-1	MSSB	F_B
Variance	SSE	(I-1)(J-1)	MSSE	
Sum	SST	IJ-1		

In the following analysis the pile spacing is taken as factor A with three values (2a, 2.5a, 3a), and the tensile stiffness of the geosynthetic, the compression modulus of soft soil, the soft soil thickness, the embankment height and the internal friction angle of the fill are taken as the Factor B in turn, and each has six values. The subsoil reaction, the SCR and the tension of the geosynthetic are taken as the test result separately.

5.2 Analysis of the influence of the parameters on the subsoil reaction

The pile spacing is taken as factor A, which is selected as 2a, 2.5a, 3a separately. Factor B is the tensile stiffness of the geosynthetic, which can be 500 kN/m, 1000 kN/m, 1500 kN/m, 2000 kN/m, 2500 kN/m, 3000 kN/m, separately. The results of the binary variance are listed in Table 10.

Table 10. Binary-variance analysis of the pile spacing and the tensile stiffness on the subsoil reaction.

Source of variance	Sum of squares	Degree of freedom	Mean square	F
Pile spacing	732.17	2	366.09	34.23
Tensile stiffness	141.68	5	28.34	2.65
Variance	106.93	10	10.69	
Sum	980.78	17		

As for the F-distribution, α is given as 5%, thus $F_{0.05}(2, 10)$ is 4.10, $F_{0.05}(5, 10)$ is 3.33. According to the analysis, $F_A > F_{0.05}(2, 10)$ and $F_B < F_{0.05}(5, 10)$, which demonstrates the remarkable influence of the pile spacing on the subsoil reaction, but the weak influence of the tensile stiffness. The influence of the pile spacing is evidently greater than that of the tensile stiffness.

The pile spacing is taken as factor A, which can be 2a, 2.5a, 3a, separately. Factor B is the compression modulus of the soft soil, which is selected as 1 MPa, 2 MPa, 3 MPa, 4 MPa, 5 MPa, 6 MPa, separately. The results of the binary variance are listed in Table 11.

Table 11. Binary-variance analysis of the pile spacing and the compression modulus of the soft soil on the subsoil reaction.

Source of variance	Sum of squares	Degree of freedom	Mean square	F
Pile spacing	752.50	2	376.25	10.58
Compression modulus	853.57	5	170.71	4.80
Variance	355.59	10	35.56	
Sum	1961.66	17		

As for the F-distribution, α is given as 5%, thus $F_{0.05}$ (2, 10) is 4.10, and F0.05(5, 10) is 3.33. According to the analysis, $F_A > F_{0.05}(2, 10)$ and $F_B < F_{0.05}(5, 10)$, which states that the compression modulus of the soft soil imposes a non-negligible influence on the subsoil reaction, but the influence of the compression modulus is not as great as that of the pile spacing.

The pile spacing is taken as the factor A, which can be 2*a*, 2.5*a*, 3*a*, separately. The Factor B is the soft soil thickness, which is selected as 5 m, 10 m, 15 m, 20 m, 25 m, and 30m, separately. The results of the binary variance are listed in Table 12.

Table 12. Binary-variance analysis of the pile spacing and the soft soil thickness on the subsoil reaction.

Source of variance	Sum of squares	Degree of freedom	Mean square	F
Pile spacing	998.86	2	499.43	52.27
Depth	1643.16	5	328.63	34.40
Variance	95.54	10	9.55	
Sum	2737.56	17		

As for the F-distribution, α is given as 5%, thus $F_{0.05}$(2, 10) is 4.10, and $F_{0.05}(5, 10)$ is 3.33. According to the analysis, $F_A > F_{0.05}(2, 10)$ and $F_B < F_{0.05}(5, 10)$, which declares that the soft soil thickness exerts a notable influence on the subsoil reaction, and the influence of the soft soil thickness is weaker than that of the pile spacing.

The pile spacing is taken as factor A, which can be 2*a*, 2.5*a*, 3*a*, separately. Factor B is the embankment height, which is selected as 1.0s, 1.5s, 2.0s, 2.5s, 3.0s, 3.5s separately. The results of the binary variance are listed in Table 13.

As for the F-distribution, α is given as 5%, thus $F_{0.05}$(2, 10) is 4.10, and $F_{0.05}(5, 10)$ is 3.33. According to the analysis, $F_A > F_{0.05}(2, 10)$ and $F_B < F_{0.05}(5, 10)$, which declares that the embankment height has a weak influence on the subsoil reaction compared with the pile

Table 13. Binary-variance analysis of pile spacing and embankment height on subsoil reaction.

Source of variance	Sum of squares	Degree of freedom	Mean square	F
Pile spacing	1711.16	2	855.53	13.92
Embankment height	564.37	5	112.87	1.84
Variance	614.42	10	61.44	
Sum	2289.85	17		

spacing. The reason is that once the full soil arching has developed in the embankment fill, the increasing load of the embankment fill is mainly supported by piles, as a result of the arching effect.

The pile spacing is taken as factor A, which can be 2*a*, 2.5*a*, 3*a*, separately. Factor B is the internal friction angle of the fill, which is selected as 20°, 30°, 35°, 40°, 50°, 60°, separately. The results of the binary variance are listed in Table 14.

Table 14. Binary-variance analysis of the pile spacing and the internal friction angle of the fill on the subsoil reaction.

Source of variance	Sum of squares	Degree of freedom	Mean square	F
Pile spacing	587.84	2	293.92	39.16
Internal friction angle	161.23	5	32.25	4.30
Variance	75.06	10	7.51	
Sum	824.13	17		

As for the F-distribution, α is given as 5%, thus $F_{0.05}$(2, 10) is 4.10, and $F_{0.05}(5, 10)$ is 3.33. According to the analysis, $F_A > F_{0.05}(2, 10)$ and $F_B < F_{0.05}(5, 10)$, which states that the internal friction angle of fill exerts a non-negligible influence on the subsoil reaction, but the influence of the pile spacing is rather greater than that of the internal friction angle of fill.

It can be drawn from the above analysis that the influence significance on the subsoil reaction of these six parameters can be expressed from strong to weak as: Pile spacing > Soft soil thickness > Compression modulus of soft soil > Internal friction angle of fill > Embankment height > Tensile stiffness of the geosynthetic.

5.3 Analysis of the influence of the parameters on the *SCR*

The pile spacing is taken as factor A, which can be 2*a*, 2.5*a*, 3*a*, separately. Factor B is the tensile stiffness of

Table 15. Binary-variance analysis of the pile spacing and the tensile stiffness of the geosynthetic on the *SCR*.

Source of variance	Sum of squares	Degree of freedom	Mean square	F
Pile spacing	125.33	2	62.66	32.64
Tensile stiffness	46.56	5	9.31	4.85
Variance	19.20	10	1.92	
Sum	191.09	17		

the geosynthetic, which is selected as 500 kN/m, 1000 kN/m, 1500 kN/m, 2000 kN/m, 2500 kN/m, and 3000 kN/m, separately. The results of the binary variance are listed in Table 15.

As for the F-distribution, α is given as 5%, thus $F_{0.05}(2, 10)$ is 4.10, and $F_{0.05}(5, 10)$ is 3.33. According to the analysis, $F_A > F_{0.05}(2, 10)$ and $F_B < F_{0.05}(5, 10)$, which demonstrates the non-negligible influence of the tensile stiffness on the *SCR*, and the influence of the pile spacing is rather greater than that of the tensile stiffness.

The pile spacing is taken as factor *A*, which can be 2*a*, 2.5*a*, 3*a*, separately. Factor *B* is the compression modulus of the soft soil, which is selected as 1 MPa, 2 MPa, 3 MPa, 4 MPa, 5 MPa, and 6 MPa, separately. The results of the binary variance are listed in Table 16.

Table 16. Binary-variance analysis of the pile spacing and the compression modulus of the soft soil on the *SCR*.

Source of variance	Sum of squares	Degree of freedom	Mean square	F
Pile spacing	134.09	2	67.04	53.333
Compression modulus	692.17	5	138.43	110.11
Variance	12.57	10	1.26	
Sum	838.83	17		

As for the F-distribution, α is given as 5%, thus $F_{0.05}(2, 10)$ is 4.10, and $F_{0.05}(5, 10)$ is 3.33. According to the analysis, $F_A > F_{0.05}(2, 10)$ and $F_B < F_{0.05}(5, 10)$, which illustrates that the influence of the pile spacing and the compression modulus of the soft soil on the *SCR* are both remarkable, and the influence of the compression modulus is greater than that of the pile spacing.

The pile spacing is taken as factor *A*, which can be 2*a*, 2.5*a*, 3*a*, separately. Factor *B* is the soft soil thickness, which is selected as 5 m, 10 m, 15 m, 20 m, 25 m, and 30 m, separately. The results of the binary variance are listed in Table 17.

Table 17. Binary-variance analysis of the pile spacing and the soft soil thickness on the *SCR*.

Source of variance	Sum of squares	Degree of freedom	Mean square	F
Pile spacing	44.33	2	22.16	9.51
Soft soil thickness	148.81	5	29.76	12.77
Variance	23.30	10	2.33	
Sum	216.44	17		

As for F-distribution, α is given as 5%, thus $F_{0.05}(2, 10)$ is 4.10, and $F_{0.05}(5, 10)$ is 3.33. According to the analysis, $F_A > F_{0.05}(2, 10)$ and $F_B < F_{0.05}(5, 10)$, which demonstrates the notable influence of the soft soil thickness and the pile spacing on the *SCR*, but the influence of the pile spacing is not as great as that of the soft soil thickness.

The pile spacing is taken as factor *A*, which can be 2*a*, 2.5*a*, 3*a*, separately. Factor *B* is the embankment height, which is selected as 1.0 s, 1.5 s, 2.0 s, 2.5 s, 3.0 s, 3.5 s, separately. The results of the binary variance are listed in Table 18.

Table 18. Binary-variance analysis of the pile spacing and the embankment height on the *SCR*.

Source of variance	Sum of squares	Degree of freedom	Mean square	F
Pile spacing	33.77	2	16.89	31.07
Embankment height	97.12	5	19.42	35.73
Variance	5.44	10	0.54	
Sum	136.33	17		

As for F-distribution, α is given as 5%, thus $F_{0.05}(2, 10)$ is 4.10, and $F_{0.05}(5, 10)$ is 3.33. According to the analysis, $F_A > F_{0.05}(2, 10)$ and $F_B < F_{0.05}(5, 10)$, which declares that the embankment height and the pile spacing both exert an evident influence on the *SCR*, and the influence of the embankment height is slightly greater than that of the pile spacing.

The pile spacing is taken as factor *A*, which can be 2*a*, 2.5*a*, 3*a*, separately. Factor *B* is the internal friction angle of the fill, which is selected as 20°, 30°, 35°, 40°, 50°, 60°, separately. The results of the binary variance are listed in Table 19.

As for F-distribution, α is given as 5%, thus $F_{0.05}(2, 10)$ is 4.10, and $F_{0.05}(5, 10)$ is 3.33. According to the analysis, $F_A > F_{0.05}(2, 10)$ and $F_B < F_{0.05}(5, 10)$, which states that the influence of the internal friction angle of fill imposes

Table 19. Binary-variance analysis of the pile spacing and the internal friction angle of fill on the *SCR*.

Source of variance	Sum of squares	Degree of freedom	Mean square	F
Pile spacing	33.77	2	16.89	31.07
Internal friction angle	97.12	5	19.42	35.73
Variance	5.44	10	0.54	
Sum	136.33	17		

a non-negligible influence on the *SCR*, and is weaker than that of the pile spacing.

It can be drawn from the above analysis that the influence significance on the *SCR* of several parameters can be expressed from strong to weak as: Compression modulus of soft soil > Soft soil thickness > Embankment height > Pile spacing > Internal friction angle of fill > Tensile stiffness of geosynthetic.

5.4 Analysis of the influence of the parameters on the tension of the geosynthetic

The pile spacing is taken as factor *A*, which can be 2*a*, 2.5*a*, 3*a*, separately. Factor *B* is the tensile stiffness of the geosynthetic, which can be 500 kN/m, 1000 kN/m, 1500 kN/m, 2000 kN/m, 2500 kN/m, and 3000 kN/m, separately. The results of the binary variance are listed in Table 20.

Table 20. Binary-variance analysis of the pile spacing and the tensile stiffness of the geosynthetic on the tension.

Source of variance	Sum of squares	Degree of freedom	Mean square	F
Pile spacing	6317.5	2	3158.747	13.27
Tensile stiffness	6042.54	5	1208.51	5.08
Variance	2380.34	10	238.03	
Sum	14740.37	17		

As for the F-distribution, α is given as 5%, thus $F_{0.05}(2, 10)$ is 4.10, and $F_{0.05}(5, 10)$ is 3.33. According to the analysis, $F_A > F_{0.05}(2, 10)$ and $F_B < F_{0.05}(5, 10)$, which demonstrates that the both the pile spacing and the tensile stiffness exert a notable influence on the tension of the geosynthetic, and the influence of the pile spacing is stronger than that of the tensile stiffness.

The pile spacing is taken as factor *A*, which can be 2*a*, 2.5*a*, 3*a*, separately. Factor *B* is the compression modulus of the soft soil, which is selected as 1 MPa, 2 MPa, 3 MPa, 4 MPa, 5 MPa, and 6 MPa, separately. The results of the binary variance are listed in Table 21.

Table 21. Binary-variance analysis of the pile spacing and the compression modulus of the soft soil on the tension.

Source of variance	Sum of squares	Degree of freedom	Mean square	F
Pile spacing	5754.29	2	2877.15	27.63
Compression modulus	3906.25	5	781.25	7.50
Variance	1041.12	10	104.11	
Sum	10701.67	17		

As for the F-distribution, α is given as 5%, thus $F_{0.05}(2, 10)$ is 4.10, and $F_{0.05}(5, 10)$ is 3.33. According to the analysis, $F_A > F_{0.05}(2, 10)$ and $F_B < F_{0.05}(5, 10)$, which declares that the compression modulus of the soft soil imposes an evident influence on the tension of the geosynthetic, but the influence of the compression modulus is not as strong as that of the pile spacing.

The pile spacing is taken as factor *A*, which can be 2*a*, 2.5*a*, 3*a*, separately. Factor *B* is the soft soil thickness, which is selected as 5 m, 10 m, 15 m, 20 m, 25 m, and 30 m, separately. The results of the binary variance are listed in Table 22.

Table 22. Binary-variance analysis of the pile spacing and the soft soil thickness on the tension.

Source of variance	Sum of squares	Degree of freedom	Mean square	F
Pile spacing	2598.37	2	1299.19	5.57
Soft soil thickness	12776.85	5	2555.37	10.95
Variance	2333.49	10	233.35	
Sum	17708.71	17		

As for the F-distribution, α is given as 5%, thus $F_{0.05}(2, 10)$ is 4.10, and $F_{0.05}(5, 10)$ is 3.33. According to the analysis, $F_A > F_{0.05}(2, 10)$ and $F_B < F_{0.05}(5, 10)$. It can be concluded that the soft soil thickness has a great influence on the tension of the geosynthetic, and the influence of the soft soil thickness is stronger than that of the pile spacing.

The pile spacing is taken as factor *A*, which can be 2*a*, 2.5*a*, 3*a*, separately. Factor *B* is the embankment height, which is selected as 1.0 s, 1.5 s, 2.0 s, 2.5 s, 3.0 s, 3.5 s separately. The results of the binary variance are listed in Table 23.

As for the F-distribution, α is given as 5%, thus $F_{0.05}(2, 10)$ is 4.10, and $F_{0.05}(5, 10)$ is 3.33. According to the analysis, $F_A > F_{0.05}(2, 10)$ and $F_B < F_{0.05}(5, 10)$, which demonstrates the weak influence of the embankment

Table 23. Binary-variance analysis of the pile spacing and the embankment height on the tension.

Source of variance	Sum of squares	Degree of freedom	Mean square	F
Pile spacing	20160.76	2	10080.38	10.16
Embankment height	9958.46	5	1991.69	2.01
Variance	9921.14	10	992.11	
Sum	40040.36	17		

height on the tension of the geosynthetic, and the influence of the pile spacing is stronger than that of the soft soil thickness.

The pile spacing is taken as factor *A*, which can be 2*a*, 2.5*a*, 3*a*, separately. Factor *B* is the internal friction angle of the fill, which is selected as 20°, 30°, 35°, 40°, 50°, and 60°, separately. The results of the binary variance are listed in Table 24.

Table 24. Binary-variance analysis of the pile spacing and the internal friction angle of the fill on the tension.

Source of variance	Sum of squares	Degree of freedom	Mean square	F
Pile spacing	3814.90	2	1907.45	41.43
Internal friction angle	11907.16	5	2381.43	51.72
Variance	460.41	10	46.04	
Sum	16182.47	17		

As for F-distribution, α is given as 5%, thus $F_{0.05}(2, 10)$ is 4.10, and $F_{0.05}(5, 10)$ is 3.33. According to the analysis, $F_A > F_{0.05}(2, 10)$ and $F_B < F_{0.05}(5, 10)$. It can be drawn that the internal friction angle of the fill exerts a great influence on the tension of the geosynthetic, and the influence of the internal friction angle is stronger than that of the pile spacing.

It can be concluded from the above analysis that the influence significance on the tension of the geosynthetic of several parameters can be expressed from large to small as: Soft soil thickness > Internal friction angle of fill > Pile spacing > Tensile stiffness of geosynthetic > Compression modulus of soft soil > Embankment height.

5.5 Suggestions for designing the *PSGR* embankment

Normally, when designing a *PSGR* embankment, how to alleviate the tension of the geosynthetic and make more load transfer to the piles attracts most of our

attention. The soft soil thickness and the compression modulus of the soft soil are hard to accommodate for the complex geological condition and the high expense. The pile spacing, the internal friction angle of the fill and the tensile stiffness are the factors that can be accommodated in the design. In order to enlarge the pile spacing, using fill material with a large internal friction angle is the most effective way, followed by adopting a geosynthetic with a high tensile stiffness.

6 CONCLUSIONS

A new theoretical method has been presented in this paper that should be a solution to an embankment of granular fill on soft soil supported by a rectangular grid of piles and geosynthetic. The method is conceptually and mathematically simple, while it takes the arching effect, the membrane effect, the subsoil reaction and the pile head settlement into consideration. The new method can not only be applied for piles seated on a firm soil layer, but also floating piles. The proposed method is verified by comparing results with the field data and was found to be in good agreement with some current analytical methods for a low embankment case. Although the proposed method is based on plane-strain conditions, using the proposed method to get a subsoil reaction and the tension of the geosynthetic, and then calculating the stress concentration ratio based on the 3d condition, is considered to be practicable. Before the calculation of stress-concentration ratio, the clear spacing ratio (*NSR*) and the height spacing ratio (*HSR*) should be considered firstly to judge the 2d or 3d condition is adopted.

Parameters research is conducted in this paper using the proposed theoretical method, including the tensile stiffness of the geosynthetic, the compression modulus of the soft soil, the soft soil thickness, the height of the embankment, the internal friction angle of the fill and the pile spacing. The influence of these parameters on the subsoil reaction, the *SCR*, and the tension of the geosynthetic are discussed in this paper.

Based on a binary-variance analysis of the non-repeatability tests, the influence significance of the pile spacing, the tensile stiffness of the geosynthetic, the compression modulus of the soft soil, the soft soil thickness, the embankment height and the internal friction angle of the fill are studied, and the results are explained as follows:

(a) As for the subsoil reaction, the influence significance of these parameters can be expressed from large to small as: Pile spacing > Soft soil thickness >

Compression modulus of soft soil > Internal friction angle of fill > Embankment height > Tensile stiffness of geosynthetic

(b) As for *SCR*, the influence significance of these parameters can be expressed from large to small as: Compression modulus of soft soil > Soft soil thickness > Embankment height > Pile spacing > Internal friction angle of fill > Tensile stiffness of geosynthetic.

(c) As for the tension of the geosynthetic, the influence significance of these parameters can be expressed from large to small as: Soft soil thickness > Internal friction angle of fill > Pile spacing > Tensile stiffness of geosynthetic > Compression modulus of soft soil > Embankment height.

In designing a piled embankment, in order to enlarge the pile spacing, using granular material with a high friction angle for the embankment fill is the most effective and economical way, rather than using a geosynthetic with a high tensile stiffness.

In this study, piles arranged in a square pattern and one layer of geosynthetic was investigated. Further research is essential for piles arranged in other patterns, for a multi-layer reinforcement piled embankment.

Acknowledgments

REFERENCES

[1]   Magan, J.P. 1994. Methods to reduce the settlement of embankments on soft clay: a review. In: Vertical and Horizontal Deformations of Foundations and Embankments. ASCE. Geotechnical Special Publication, pp. 77-91.

[2]   Liu, H.L., Charles, W.W.Ng., Fei, K. 2007. Performance of a geogrid-reinforced and pile-supported highway embankment over soft clay: case study. Journal of Geotechnical and Geoenvironmental Engineering 133, 12, 1483-1493. DOI: 10.1061/(ASCE)1090-0241(2007)133:12(1483)

[3]   Han, J., Gabr, M.A. 2002. Numerical analysis of geosynthetic-reinforced and pile-supported earth platforms over soft soil. Journal of Geotechnical and Geoenvironmental Engineering 128, 1, 44-53. DOI: 10.1061/(ASCE)1090-0241(2002)128:1(44)

[4]   Gangakhedkar, R. 2004. Geosynthetic Reinforced Pile Supported embankments. University of Florida, Florida.

[5]   Almeida, M.S.S., Ehilich, M., Spotti, A.P., Marques, M.E.S. 2007. Embankment supported on piles with biaxial geogrids. Geotechnical Engineering 160, 4, 185-192. DOI: 10.1680/geng.2007.160.4.185

[6]   Van Eekelen, S.J.M., Bezuijen, A., Alexiew, D. 2008. Piled embankments in the Netherlands, a full-scale test, comparing 2 years of measurements with design calculation. Proc. EuroGeo4, pp. 264.

[7]   Briancon, L., Simon, B. 2012. Performance of pile-supported embankment over soft soil: full-scale experiment. Journal of Geotechnical and Geoenvironmental Engineering 138, 4, 551-561. DOI: 10.1061/(ASCE)GT.1943-5606.0000561

[8]   Van Eekelen, S.J.M.V., Bezuijen, A., Tol, A.F.V. 2013. An analytical model for arching in piled embankments. Geotextiles and Geomembranes 39, 78-102. DOI: 10.1016/j.geotexmem.2013.07.005

[9]   Carlsson, B. 1987. Reinforced Soil, Principles for Calculation. Terratema AB, Linköping (in Swedish).

[10] Guido, V.A. Kneuppel, J.D., Sweeny, M.A. 1987. Plate loading test on geogrid-reinforced earth slabs. In: Proceedings of geosynthetics'87, New Orleans, USA. IFAI, pp. 216-225.

[11] Hewlett, W.J., Randolph, M.F. 1988. Analysis of piled embankment. Ground Engineering 21, 3, 12-18.

[12] Low, B.K., Tang, S.K., Choa, V. 1994. Arching in piled embankment. Journal of Geotechnical Engineering 120, 11, 1917-1938. DOI: 10.1061/(ASCE)0733-9410(1994)120:11(1917)

[13] Collin, J.G. 2004. Column supported embankment design consideration. In: 52nd Annual Geotechnical Engineering Conference. University of Minnesota.

[14] Raithel, M., Kirchner, A., Kempfert, H.G. 2008. German recommendations for reinforced embankments on pile-similar elements. Proc. 4th Asian Regional Conference on Geosynthetics, Shanghai, pp. 697-702.

[15] Terzaghi, K., 1943. Theoretical soil mechanics. John Wiley and Sons, New York.

[16] Chen, R.P., Chen, Y.M., Xu, Z.Z. 2008a. A theoretical solution for pile-supported embankments on soft soils under one-dimensional compression. Canadian Geotechnical Engineering 45, 6, 611-623. DOI: 10.1139/T08-003

[17] Lu, W.H., Miao, L.C. 2015. A simplified 2-D evaluation method of the arcing effect for geosynthetic-reinforced and pile-supported embankments. Computers and Geotechnics 65, 97-103. DOI: 10.1016/j.compgeo.2014.11.014

[18] BS8006-1-2010. Code of Practice for Strengthened/Reinforced Soils and Other Fills. British Standard Institution, 2010.

[19] Zhang, C.L., Jiang, G.L., Liu, X.F., Buzzi, O. 2016. Arching in geogrid-reinforced pile-supported embankments over silty-clay of medium compressibility: Field data and analytical solution. Computers and Geotechnics 77, 11-25. DOI: 10.1016/j.compgeo.2016.03.007

[20] Abushrar, S.W., Zheng, J.J., Chen, B.G., Yin, J.H. 2009. A simplified method for analysis of a piled embankment reinforced with geosynthetic. Geotextiles and Geomembranes 27, 1, 39-52. DOI: 10.1016/j.geotexmem.2008.05.002

[21] Filz, G., Sloan, J. 2013. Load distribution on geosynthetic reinforcement in column-supported embankments. Geo-congress, 231, pp. 1822-1830.

[22] Zhuang, Y., Wang, K.Y., Liu, H.L. 2014. A simplified model to analyze the reinforced piled embankments. Geotextiles and Geomembranes 42, 2, 154-165. DOI: 10.1016/j.geotexmem.2014.01.002

[23] Russell, D., Naughton, P.J., Kempton, G. 2003. A new design procedure for piled embankments. Proc. 56th Canadian Geotechnical Conf. and 2003 NAGS Conf., pp. 858-865.

[24] Yu, C., Liu, S.Y., Ji, T.Y. 2006. Study on the performance of the reinforced piled embankment. ASCE Geotechnical Special Publication, 151, pp. 247-254.

[25] Jones, C. 1990. Geotextile reinforced piled embankments. Proc. 4th Int. Conf. on Geotextiles: Geomembranes and Related products. Rotterdam: Balkema, pp. 155-160.

[26] Yasufuku, N., Hyde, A.F.L. 1995. Pile end-bearing capacity in crushable sands. Geotechnique 45, 1, 663-676.

[27] Liu, J.F. 2011. Study on working mechanism and calculation method of settlement control for railway's roadbed using CFG-pile composite foundation. Southwest Jiaotong University, Chengdu.

[28] JGJ 94-2008: 2008. 2008. Technical code for building pile foundations. China Architecture & Building Press, Beijing.

[29] Vesic, A.S. 1977. Design of pile foundation. National Cooperative Highway Research Program Synthesis of Practice, Washington.

[30] Van Eekelen, S.J.M.V., Bezuijen, A., Tol, A.F.V. 2015. Validation of analytical models for the design of basal reinforced piled embankments. Geotextiles and Geomembranes 43, 1, 56-81. DOI: 10.1016/j.geotexmem.2014.10.002

[31] Chen, R.P., Xu, Z.Z., Chen, Y.M., Ling, D.S., Zhu, B. 2010. Field tests on pile-supported embankments over soft ground. Journal of Geotechnical and Geoenvironmental Engineering 136, 6, 777-785. DOI: 10.1061/(ASCE) GT1943-5606.0000295

[32] Chen, Y.M., Cao, W.P., Chen, R.P. 2008b. An experimental investigation of soil arching within basal reinforce and unreinforced piled embankments. Geotextiles and Geomembranes 26, 2, 164-174. DOI: 10.1016/j.geotexmem. 2007.05.004

[33] Hello, B.L., Villard, P. 2009. Embankment reinforced by piles and geosynthetics-Numerical and experimental studies dealing with the transfer of load on the soil embankment. Engineering Geology 106, 1-2, 78-91. DOI: 10.1016/j.enggeo.2009.03.001

[34] Wang, R.X. 2005. Mathematical Statistics. Xi An Jiaotong Univesity Press, Xi An.